Catalysis
Science & Technology

RSC Publishing

PAPER

View Article Online
View Journal

Cite this: DOI: 10.1039/c3cy00238a

Au/xCeO$_2$/Al$_2$O$_3$ catalysts for VOC elimination: oxidation of 2-propanol

Pandian Lakshmanan,[a] Laurent Delannoy,[b] Catherine Louis,[b] Nicolas Bion[a] and Jean-Michel Tatibouët*[a]

Received 12th April 2013,
Accepted 5th July 2013

DOI: 10.1039/c3cy00238a

www.rsc.org/catalysis

2-Propanol oxidation (1 mol% in air) was investigated over 1%Au/CeO$_2$, 1%Au/Al$_2$O$_3$ and 1%Au/xCeO$_2$/Al$_2$O$_3$ (x = 1.5, 3, 5 and 10 wt%) catalysts and the corresponding pure supports. The effects of the catalyst activation procedure (calcination or reduction), cerium oxide morphology and loading, the presence/absence of O$_2$ in the feed, and stability of activity were studied. The nature of the support strongly influences the 2-propanol oxidation pathway, and one can distinguish three reaction temperature ranges: low (50–150 °C), intermediate (175–250 °C) and high (>300 °C). In the low temperature range, only acetone is formed whatever the nature of the support. On Au/Al$_2$O$_3$ and Au/xCeO$_2$/Al$_2$O$_3$ catalysts propene becomes the main reaction product by increasing the temperature, followed by CO$_2$ formation at higher temperature. The acidic character of Al$_2$O$_3$ and CeO$_2$/Al$_2$O$_3$ promotes the propene formation whereas the basic one of CeO$_2$ favors the formation of acetone, and the gold catalysts also present an acidic–basic behavior, which depends largely on the reaction temperature. Replacing air with He during the catalytic run over Au/Al$_2$O$_3$ and Au/CeO$_2$ provides evidence of how O$_2$ is activated by Au, revealing, as expected, that dehydrogenation to form acetone and total oxidation to CO$_2$ require both O$_2$ and Au as the catalyst, whereas dehydration to form propene does not require O$_2$. For both calcined and reduced catalysts, the catalytic activity towards total oxidation varies in the order: Au/CeO$_2$ > Au/xCeO$_2$/Al$_2$O$_3$ > Au/Al$_2$O$_3$.

1. Introduction

Au nanoparticles supported on cerium oxide surfaces present interesting catalytic applications derived from the versatile redox properties of cerium oxide and its interaction with gold. Important applications include catalytic combustion of volatile organic compounds (VOCs),[1–7] low-temperature water-gas shift (LT-WGS) reaction[8,9] and preferential oxidation of CO (PROX).[10] CeO$_2$ is well known for its unique property, namely its ability to shift between two oxidized states ($Ce^{3+} \leftrightarrow Ce^{4+}$) and to accommodate variable levels of bulk and surface oxygen vacancies.[11] The interaction between Au and CeO$_2$ is intimate and the electronic state of gold is critically influenced by the structure and morphology of cerium oxide.[6–10,12–15] In 1%Au/CeO$_2$ (S_{BET} 200 m^2 g^{-1}) gold exists in oxidized form (Au^{3+}) after calcination and in reduced form (Au^0) after reduction with hydrogen.[6] At higher Au loadings, nanosized CeO$_2$ particles stabilize small gold clusters or gold ions, which may even be incorporated into the cerium oxide nanoparticles at higher temperatures.[16] The incorporation of gold ions into the ceria lattice can generate both electronic and geometric effects. Cerium oxide crystallizes in the fluorite structure with a face-centered cubic (fcc) unit cell.[11] In this structure, each cerium cation (Ce^{4+}, ionic radii 0.097 nm)[17] is coordinated to the 8 nearest oxygen anions at the corner of a cube. If a trivalent cation (in the present study: Au^{3+} ionic radii 0.085 nm)[17,18] is introduced into the ceria lattice, extrinsic oxygen vacancies can be formed by a charge-compensating mechanism.[11,17] The difference between the cationic radii of Ce^{4+} and Au^{3+} eventually allows the compensation of the volume increase when the Ce^{4+} cation is reduced to Ce^{3+} (0.114 nm)[17] thus facilitating this reduction, as already observed for Zr^{4+} in the ceria lattice.[11,19] In fact, the presence of gold enhances the reducibility of ceria surface oxygen[8,20,21] by weakening the Ce–O bonds adjacent to gold atoms, leading to the activation of surface capping oxygen.[2,3,8,22–24] Therefore, the nature of the ceria surface with which gold interacts can greatly influence the oxidation state, size, and distribution of gold in the catalysts.

[a] Institut de Chimie des Milieux et Matériaux de Poitiers (IC2MP) UMR CNRS 7285, Université de Poitiers, Ecole Nationale Supérieure d'Ingénieurs de Poitiers, 1, rue Marcel Doré, 86022 Poitiers cedex, France. E-mail: jean.michel.tatibouet@univ-poitiers.fr
[b] Laboratoire de Réactivité de Surface (LRS), UMR CNRS 7197, Université Pierre et Marie Curie, 4 place Jussieu, 75252 Paris cedex 5, France

Although the effects of morphology of ceria for gold catalysts have been already studied,[13] ceria is usually not used as a support due to its poor resistance against thermal sintering. CeO_2 is often supported on an oxide support, such as Al_2O_3, to obtain CeO_2–Al_2O_3 mixed oxides.[25] Depending upon the ceria loading on alumina, three-dimensional particles (3D-CeO_2) and two-dimensional ceria layers (2D-CeO_2) can be formed, their redox properties differing from that of unsupported ceria.[26,27] Such variations in the morphology of alumina-supported ceria affected the distribution of gold between alumina and ceria surfaces, the redox properties of ceria and then the catalytic activity of gold based catalysts.[7]

Based on this background, the present study was undertaken to study the 2-propanol oxidation reaction on various gold based catalysts containing 1 wt% of Au loaded on unsupported ceria, pure alumina and alumina-supported ceria with different ceria loadings. The reaction conditions are close to those of VOC elimination, *i.e.*, 2-propanol is highly diluted in air. The catalytic results are discussed in terms of mechanistic formation of acetone and propene related to the oxidation state of gold.[28–32]

2. Experimental

Pure alumina (AluC Degussa, 110 $m^2\ g^{-1}$) was used as a support to load cerium oxide (1.5, 3, 5 and 10 wt% with respect to alumina) by impregnation in excess of an aqueous solution of $Ce(NO_3)_3{\cdot}6H_2O$ (Aldrich, 99.9%). 1 wt% of gold was loaded on the various CeO_2–Al_2O_3 samples by deposition–precipitation with urea. The details of experimental procedures regarding catalyst preparation, and characterization by elemental analyses, BET surface area analysis, XRD, XPS and combined TEM-EFTEM techniques were largely described in our previous study.[7] Catalysts are named Au/CeO_2 and Au/Al_2O_3 for 1 wt% Au supported on pure CeO_2 and Al_2O_3, and Au/$x$$CeO_2$/$Al_2O_3$ for 1 wt% Au on Al_2O_3 support containing x wt% of CeO_2 (Table 1). Before use, catalysts were either activated under an air flow at 400 °C (calcination) or under pure H_2 at 300 °C (reduction) (100 mL min^{-1}, 2 °C min^{-1} from room temperature to the final temperature then 2 h at the final temperature). Note that for the sake of brevity, these treatments are called calcinations and reductions, respectively, in the following.

2-Propanol oxidation was carried out in a flow-type packed bed tubular micro-reactor (inner diameter 3 mm) with 10 mg of the catalyst. The 2-propanol concentration was 1 mol% in air (total gas flow rate of 50 mL min^{-1}). The reaction temperature was increased stepwise from room temperature to 400 °C at a heating rate of 1 °C min^{-1} with a 2 h temperature plateau every 25 or 50 °C. Catalytic activity at each temperature was measured after the steady-state was reached (30–40 min). No deactivation was observed during the measurement at each plateau of temperature (2 h). After obtaining three consistent analyses, the temperature was increased to the next plateau.

The analysis of 2-propanol and the various products (acetone, propene, CO, CO_2 and ethane) was performed using a gas chromatograph (Perkin-Elmer AutoSystem) equipped with a Porapak-R column (1.8 m, 3.17 mm o.d), and a Carboxen-1000 column (4.5 m, 3.1 o.d).

For the purpose of comparison, pure supports without gold loading were also tested under similar reaction conditions. The reproducibility of the catalytic results was carefully checked. Effects of the catalyst activation method, ceria loading, and the presence/absence of O_2 in the feed were investigated. The effect of the presence/absence of O_2 in the reactant flow was investigated at a temperature at which both acetone and propene form. During the catalytic run, air was replaced by He at steady state under similar reaction conditions, and the gas composition exiting the reactor was analyzed as a function of time-on-stream. After running reaction under He, again He was replaced by air to verify the reversibility.

Table 1 Elemental analyses and the average gold particle size for various catalysts

	Elemental analysis (wt%)		Au particle size (nm)	
Catalyst	Au	CeO_2	Calcination	Reduction
Au/CeO_2	0.97	98.3	n.m	n.m
Au/1.5CeO_2/Al_2O_3	0.93	1.41	2.6 (0.55)[a]	2.3 (0.52)
Au/3CeO_2/Al_2O_3	0.99	2.64	2.7 (0.53)	2.3 (0.45)
Au/5CeO_2/Al_2O_3	0.89	4.26	2.6 (0.43)	2.2 (0.47)
Au/10CeO_2/Al_2O_3	0.89	8.06	2.6 (0.57)	2.0 (0.45)
Au/Al_2O_3	0.88	—	2.4 (0.56)	2.0 (0.49)

n.m – not measurable.[a] Standard deviation.

3. Results and discussion

3.1. Summary of the characterization study of the catalysts

First, a summary of the characterization study performed earlier on these catalysts[7] is presented here. The morphology of alumina-supported ceria varied according to the ceria loading. In agreement with Arias's results,[27] it was proposed that up to 3 wt% CeO_2 on alumina, ceria clusters are mainly as 2-D patches and that above this loading, 3-D CeO_2 nanoparticles begin to appear, as shown by the results of XRD and TEM. In 5CeO_2/Al_2O_3 and 10CeO_2/Al_2O_3 samples, 3-D CeO_2 nanoparticles ($\sim$8 nm) are present. These variations in the morphology of ceria affected the characteristics of the gold nanoparticles in terms of their distribution between alumina and ceria, oxidation state, and average particle size. As the ceria loading increased (1.5, 3, 5, and 10 wt% CeO_2), the percentage of gold particles visible in the TEM micrographs decreased while the particle size did not change, and since the gold particles are visible on alumina and not on ceria because of the poor contrast between gold and ceria, it was deduced that the percentage of gold particles on ceria increased as the ceria loading increased. Energy filtered TEM (EFTEM) confirmed that gold particles were in close contact with ceria particles. The XPS analyses of Au/CeO_2/Al_2O_3 catalysts carried out at liquid nitrogen temperature revealed that the oxidation state of gold depended upon the ceria loading and the type of catalyst activation (calcination or reduction). Gold on pure Al_2O_3 was in metallic state, whatever the activation treatment, whereas gold on pure ceria was metallic only after reduction,

most of the gold remaining unreduced after calcination; interaction between gold and ceria stabilizes gold in a higher oxidation state. Consistently, the XPS results also showed that in the reduced Au/xCeO$_2$/Al$_2$O$_3$ samples, gold was metallic as on pure alumina and ceria whereas in calcined samples the results depended on the CeO$_2$ loading.

Finally, the average size of the gold particles visible by TEM is in general smaller after reduction treatment than after calcination (Table 1).

3.2. Oxidation of 2-propanol

As a blank experiment, 2-propanol oxidation was conducted in the empty reactor. The thermal decomposition of 2-propanol begins around 325 °C. At 400 °C, 23% of 2-propanol was converted into acetone (94%), propene (4%) and carbon dioxide (2%).

Fig. 1 compares the catalytic performances of calcined (Fig. 1B) and reduced (Fig. 1C) Au/CeO$_2$ along with those of the pure CeO$_2$ support (Fig. 1A). Acetone forms at low temperature over pure CeO$_2$ due to the basic nature of ceria. Ceria is also active for the total oxidation of 2-propanol to CO$_2$ at higher temperature since at 200 °C, 2-propanol is completely converted into CO$_2$ (Fig. 1A). The addition of gold decreases the temperature at which 2-propanol is totally converted: ~150 °C for calcined or reduced Au/CeO$_2$ (Fig. 1B and C) compared to 200 °C for pure ceria. One can note that at low temperature, reduced Au/CeO$_2$ is more active than calcined one.

Fig. 2 compares the catalytic performances of Au/Al$_2$O$_3$ samples after calcination (Fig. 2B), reduction (Fig. 2C) and the pure calcined Al$_2$O$_3$ support (Fig. 2A). On pure alumina, 2-propanol undergoes dehydration and forms propene due to its acidic character. 2-Propanol is completely converted into propene around 200 °C, and the CO$_2$ formation at higher temperature is very low: 6% at 400 °C with 2% CO. By contrast, the presence of gold on Al$_2$O$_3$ changes completely the catalytic behavior of 2-propanol transformation. Whatever the catalyst treatment (calcination or reduction), acetone instead of propene is formed on Au/Al$_2$O$_3$ catalysts at low temperature (Fig. 2B and C). At temperatures higher than 175 °C, and at about 100% of 2-propanol conversion, propene gradually appears at the expense of acetone and reaches a maximum at about 350 °C, while the CO$_2$ formation remains low. For the calcined sample, the propene starts to form at lower temperature and reaches higher selectivity than for the reduced sample. These results show the poor performance of the Au/Al$_2$O$_3$ catalyst compared to Au/CeO$_2$ towards the total oxidation of 2-propanol, but reveal the capacity of Au/Al$_2$O$_3$ to act as a selective oxidation catalyst. One can distinguish three reaction temperature regions: dehydrogenation of 2-propanol to acetone (50–150 °C), dehydration to propene (175–250 °C) and total oxidation to CO$_2$ (>350 °C).

Fig. 3 reports the catalytic results obtained for the pure calcined 10CeO$_2$/Al$_2$O$_3$ support (Fig. 3A), calcined (Fig. 3B) and reduced (Fig. 3C) Au/10CeO$_2$/Al$_2$O$_3$ samples. The pure 10CeO$_2$/Al$_2$O$_3$ support exhibits roughly the same behavior as Al$_2$O$_3$ (Fig. 2A). 2-Propanol undergoes dehydration to form propene above 150 °C. Complete conversion to propene is reached at about 200 °C (Fig. 3A) without any formation of acetone although ceria particles are present.

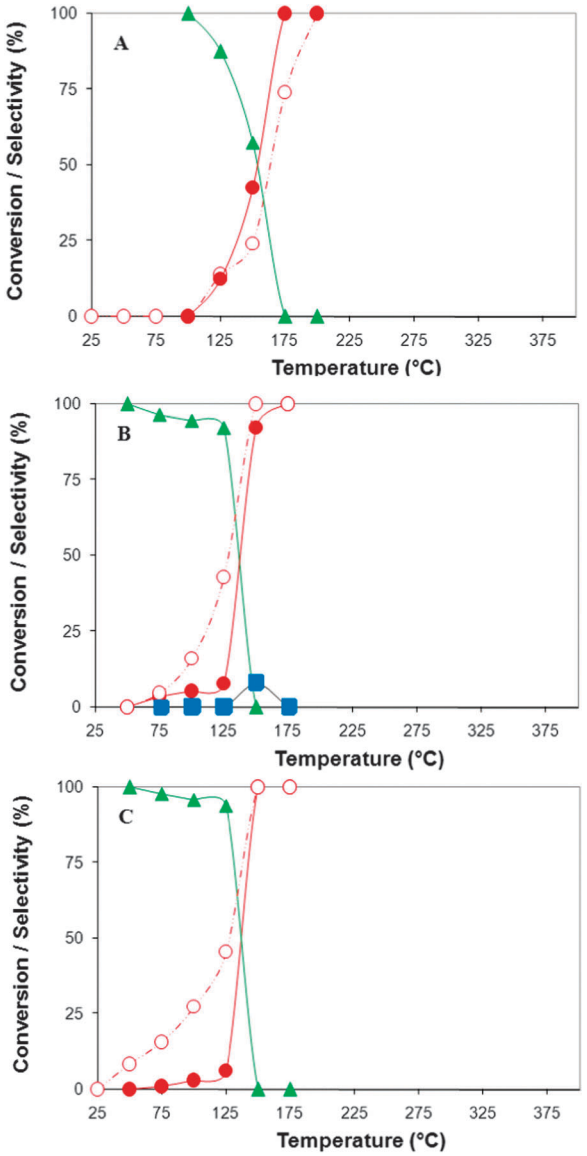

Fig. 1 Conversion of 2-propanol (○) and products distribution (▲ – acetone; ● – CO$_2$; ■ – propene) on a pure CeO$_2$ support (A); calcined (B) and reduced Au/CeO$_2$ (C).

The calcined Au/10CeO$_2$/Al$_2$O$_3$ catalyst exhibits a catalytic behavior rather similar to that of Au/Al$_2$O$_3$ (Fig. 2B and C) except that it is more active, and the curves are drastically shifted to lower temperatures. In the low temperature region, acetone is formed exclusively up to 125 °C, followed by a progressive decrease in the selectivity to acetone and an increase in the selectivity to propene, which passes through a maximum at 225 °C instead of 350 °C for calcined Au/Al$_2$O$_3$. The reduced Au/10CeO$_2$/Al$_2$O$_3$ sample behaves very differently from the calcined one, and rather behaves like the reduced Au/CeO$_2$ catalyst (Fig. 1C) The formation of propene is very weak between 175 and 225 °C, and CO$_2$ becomes the main product at temperature as low as 225 °C.

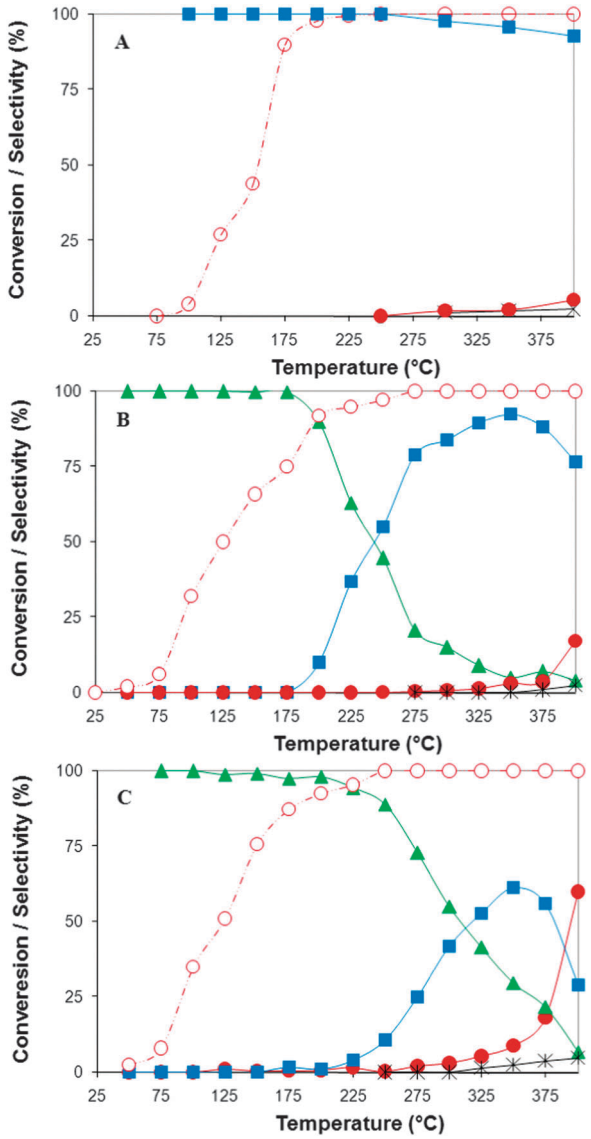

Fig. 2 Conversion of 2-propanol (○) and products distribution (▲ – acetone; ● – CO_2; ■ – propene, ×-CO) on a pure Al_2O_3 support (A); calcined (B) and reduced Au/Al_2O_3 (C).

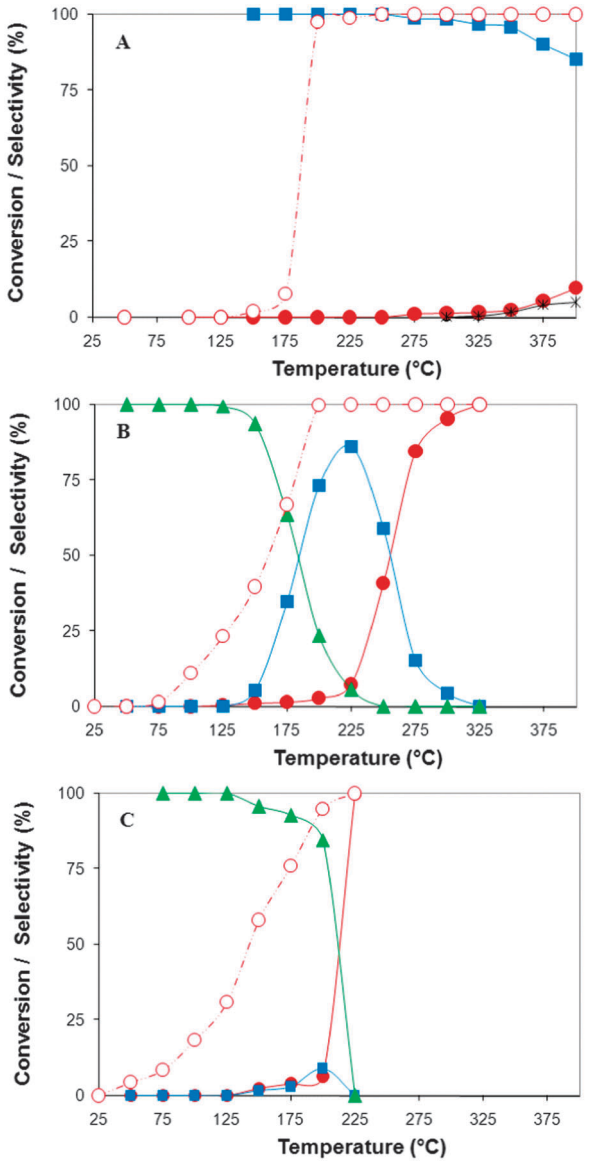

Fig. 3 Conversion of 2-propanol (○) and products distribution (▲ – acetone; ● – CO_2; ■ – propene; ×-CO) on a pure $10CeO_2/Al_2O_3$ support (A); calcined (B) and reduced $Au/10CeO_2/Al_2O_3$ (C).

If the nature of the pretreatment does not modify the temperature dependence of 2-propanol conversion to a large extent, the reduced $Au/10CeO_2/Al_2O_3$ catalyst is much more active for the total oxidation of 2-propanol. Indeed, at ~225 °C, 100% conversion is obtained for both catalysts, but at this temperature, the CO_2 selectivity is close to 100% for the reduced one whereas for the calcined one, selectivities to CO_2 and propene are 7% and 85%, respectively, and 100% of CO_2 selectivity is reached at 325 °C, only. Moreover, the formation of propene on reduced $Au/10CeO_2/Al_2O_3$ is very weak between 175 and 225 °C, and acetone is the main product.

Hence, the catalytic results obtained with $Au/10CeO_2/Al_2O_3$ indicate that gold on ceria is more active in total oxidation of 2-propanol when gold is in the metallic state than when it is unreduced (calcined), which is in agreement with our previous studies on CO and propene oxidation.[7]

The catalytic behavior of the $Au/1.5CeO_2/Al_2O_3$ catalyst resembles closely the one of $Au/10CeO_2/Al_2O_3$ with however a lower selectivity to propene in the intermediate temperature range for the calcined sample. The two other samples of intermediate ceria loadings, $Au/3CeO_2/Al_2O_3$ and $Au/5CeO_2/Al_2O_3$ catalysts, behave in between. The product distribution of $Au/3CeO_2/Al_2O_3$ resembles closely that of $Au/1.5CeO_2/Al_2O_3$ whereas the behavior of $Au/5CeO_2/Al_2O_3$ is close to that of $Au/10CeO_2/Al_2O_3$.

As can be seen from the figures of the calcined Au/CeO_2 and $Au/10CeO_2/Al_2O_3$ samples (Fig. 1B and 3B), the fall of selectivity to acetone when the temperature is increased corresponds to the maximum selectivity to propene. One can therefore wonder whether acetone is an intermediate for the formation of propene. To verify that, the reaction of acetone oxidation was conducted under similar reaction conditions. Whatever the catalyst, CO_2 was

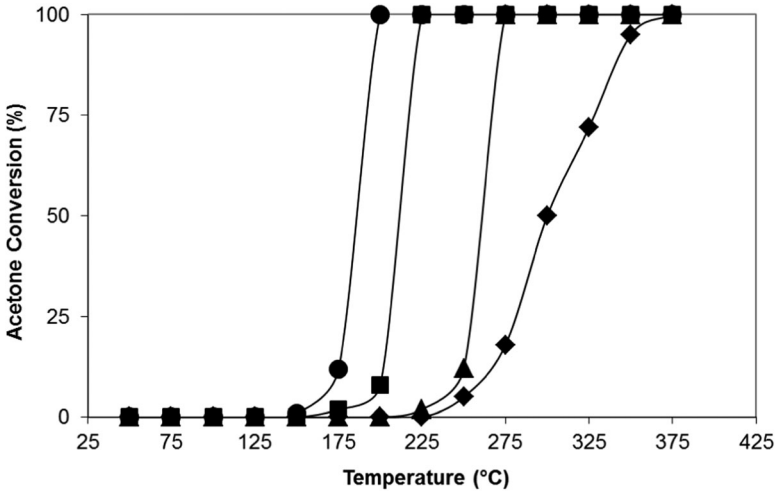

Fig. 4 Conversion of acetone on various catalysts (● – Au/CeO_2; ■ – $Au/10CeO_2/Al_2O_3$; ▲ – $Au/1.5CeO_2/Al_2O_3$; ♦ – Au/Al_2O_3).

the only product obtained and propene was not formed. Hence, one can conclude that propene directly arises from 2-propanol oxidation and not from acetone; this demonstrates the existence of two different reaction pathways for the formation of propene and acetone. The light-off curves for acetone oxidation (Fig. 4) show that the activity order determined at 50% conversion is the following: $Au/CeO_2 > Au/10CeO_2/Al_2O_3 > Au/1.5CeO_2/Al_2O_3 > Au/Al_2O_3$.

3.3. Effect of the presence/absence of O_2 in the feed

It has been shown above that, when they are calcined in air, the pure Al_2O_3 and CeO_2/Al_2O_3 supports (Fig. 2A and 3A) mainly transform 2-propanol into propene, while the pure CeO_2 and all the gold catalysts exclusively form acetone, suggesting a crucial role of Au in the dehydrogenation reaction of 2-propanol into acetone.

In order to better understand how the supports interact with gold or participate in the catalytic process, we studied the catalytic 2-propanol transformation in the absence of oxygen for reduced Au/CeO_2 and Au/Al_2O_3. Reduction pre-treatment was selected based on the fact that Au^0 is expected to be the catalytically active species for the CO oxidation reaction,[6] so the replacement of air by helium should make it possible to determine if the oxygen species needed for the reaction come from the gas phase or *via* the support. The reaction temperature was chosen to correspond to the one at which the selective formation of acetone begins to shift to CO_2 (on Au/CeO_2) or to propene (on Au/Al_2O_3) with air, *i.e.* 125 °C for reduced Au/CeO_2 and 225 °C for reduced Au/Al_2O_3.

Fig. 5A shows the evolution of the product distribution during 2-propanol conversion at 125 °C over reduced Au/CeO_2 as a function of the nature of carrier gas, air or He. After 2.5 hours during which 2-propanol in air and at 125 °C converts into acetone and into CO_2 to a very small extent, in agreement with the results presented in Fig. 1C, the air flow is replaced by He. Gradually, the conversion of 2-propanol falls down and reaches zero after 4 hours. Meanwhile, the CO_2 production stops within 2 hours and the acetone formation within 4 hours, (Fig. 5A).

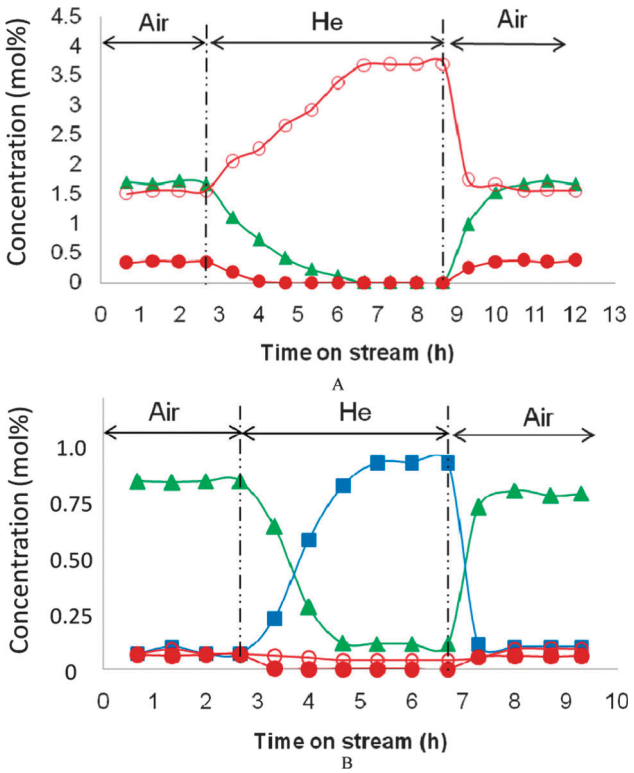

Fig. 5 Effect of replacement of air by He during 2-propanol oxidation with reduced Au/CeO_2 at 125 °C (A); reduced Au/Al_2O_3 at 225 °C (B). The changes in the distribution of products: ○-2-propanol; ▲ – acetone; ■ – propene; ● – CO_2.

If the remaining air (in large excess compared to 2-propanol) resulting from the slow purge of the whole experimental set-up certainly contributes to the slow decrease of conversion, the fact that CO_2 formation collapses much more rapidly than acetone formation allows us to conclude that the reaction of oxidative dehydrogenation of 2-propanol into acetone involves the contribution of oxygen released from the readily reducible ceria, indicating a Mars and van Krevelen-type reaction mechanism;

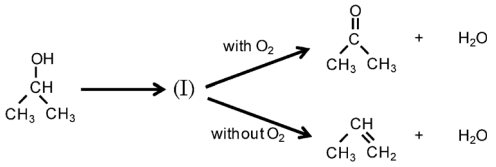

Scheme 1 Reaction scheme for the Au/Al_2O_3 catalyst.

the oxygen storage/release capacity (OSC) of ceria is well known,[11] and the occurrence of the Mars and van Krevelen mechanism was proposed by Nieuwenhuys *et al.*[15] to explain the catalytic activity in propene total oxidation of Au/CeO_2–Al_2O_3 catalysts under an Ar flow. Conversely, when He is replaced by air flow after 6.5 hours (Fig. 5A), the initial conversion is recovered much faster within around 2 hours with the same proportion of acetone and CO_2 as initially because of the easy replenishment of oxygen-depleted ceria by oxygen of the gas phase.

When the same experiment is performed over the reduced Au/Al_2O_3 catalyst at 225 °C, acetone is the main product in the presence of air, along with very small amounts of propene and CO_2 (Fig. 5B), in agreement with the results in Fig. 2C. When air is replaced by He, there is no significant change in the conversion of 2-propanol but selectivity drastically changes, and acetone and CO_2 formation is replaced by propene formation. Again these changes are totally reversible when air is reintroduced. This behavior indicates that in the absence of oxygen, the catalyst behaves like pure alumina (Fig. 2A), *i.e.* as a dehydrating catalyst, and that gold does not play any role. In contrast, the different selectivity in the presence of O_2 in the gas phase indicates that activation of oxygen requires the presence of Au^0 nanoparticles. Moreover, the same 2-propanol conversion with or without oxygen in the gas phase, but with a totally different selectivity (acetone with oxygen, propene without oxygen) could indicate that the rate limiting step for these two reactions is the formation of a common intermediate species, this intermediate species being transformed into acetone in the presence of oxygen and into propene in the absence of oxygen (Scheme 1).

According to this interpretation, the selectivity change from acetone to propene when the reaction temperature increases in the presence of oxygen on Au/Al_2O_3 catalysts (Fig. 2B and C) could be explained by the decreasing ability of gold particles to participate in the activation of oxygen when the reaction temperature increases, thus favoring propene formation at the expense of acetone formation.

3.4. General reaction scheme of 2-propanol oxidation over $Au/CeO_2/Al_2O_3$ catalysts

A model describing the catalytic behavior of the Au/CeO_2–Al_2O_3 catalysts can be proposed on the basis of the respective behavior of the Au/CeO_2 and Au/Al_2O_3 catalysts (Scheme 2). We have to distinguish three reaction temperature domains: low (50–150 °C), intermediate (175–250 °C) and high (> 250 °C). In the low temperature domain, and whatever the catalyst pretreatment (calcination or reduction), the single reaction

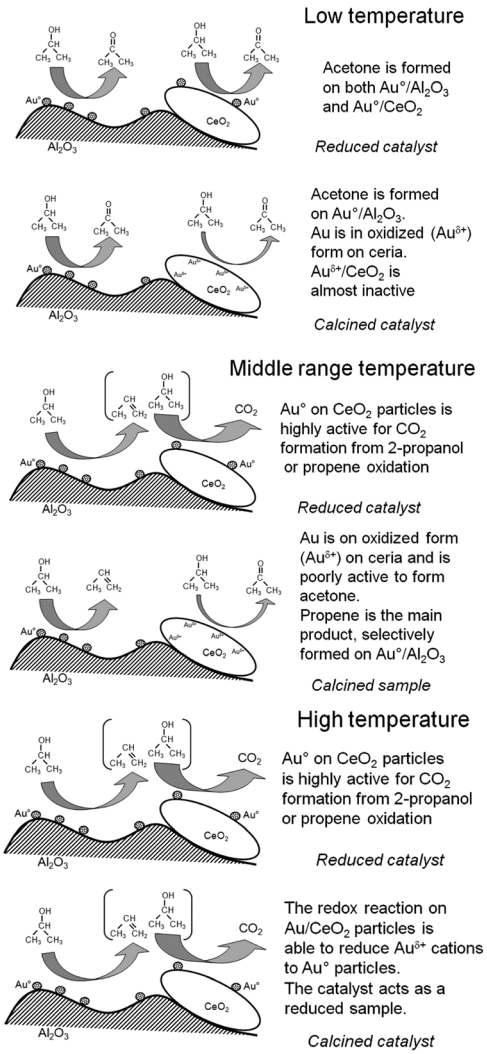

Scheme 2 General reaction scheme for $Au/CeO_2/Al_2O_3$ reduced and calcined catalysts.

product is acetone over $Au/CeO_2/Al_2O_3$ although in the reduced sample gold is in metallic form (Au^0) while in the calcined sample, gold is metallic (Au^0) on alumina but mainly in ionic form ($Au^{\delta+}$) on ceria particles (see Section 3.1). This behavior is the same as the one observed on Au/Al_2O_3 and Au/CeO_2 catalysts in the same temperature domain (Fig. 1B and C and 2B and C). However if one examines more closely the activities at 125 °C for the set of $Au/CeO_2/Al_2O_3$ catalysts (Fig. 6), one can distinguish differences between the reduced and calcined samples, and according to the ceria loading: the reduced samples are more active than the calcined ones, and the activity of the reduced ones increases as the ceria loading increases while this follows the opposite trend for the calcined samples. Since when the ceria loading increases, the amount of gold interacting with ceria also increases (see Section 3.1), leading to a decreasing amount of metallic Au interacting with alumina, the lower catalytic activity of the calcined samples indicates that the presence of $Au^{\delta+}$ in the samples (on the ceria particles) is detrimental for the activity. Moreover, one can also deduce

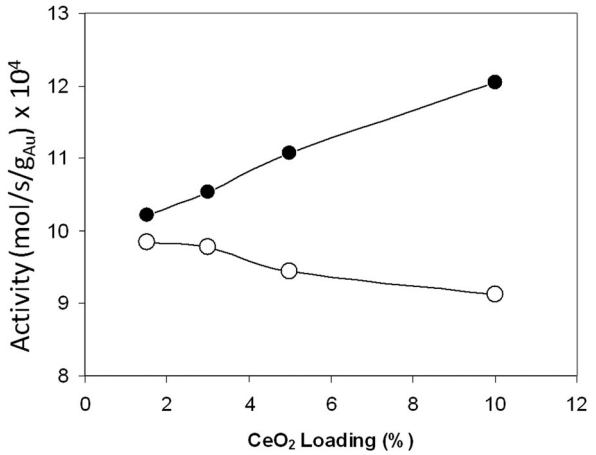

Fig. 6 Variation of activity measured at 125 °C over $Au/CeO_2/Al_2O_3$, as a function of the ceria loading and catalyst activation method for various catalysts: ○ – calcination; ● – reduction.

from Fig. 6 that Au^0 on ceria particles is more catalytically active than Au^0 on alumina since the catalytic activity of the reduced samples, where all the gold is metallic, increases with the ceria content.

In the intermediate temperature domain, the reduced $Au/CeO_2/Al_2O_3$ catalysts lead mainly to CO_2 formation and the calcined ones lead to propene formation with a maximum of selectivity in propene around 225 °C. The only difference between the reduced and calcined $Au/CeO_2/Al_2O_3$ catalysts that can explain the different selectivities in this intermediate temperature domain is the oxidation state of the gold interacting with the ceria particles. Moreover, the similarity of catalytic behavior between calcined $Au/CeO_2/Al_2O_3$ and Au/Al_2O_3 indicates that $Au^{\delta+}/CeO_2$ is poorly active in 2-propanol transformation. In the reduced Au/CeO_2–Al_2O_3 catalyst, gold is metallic (Au^0) both on alumina and ceria, and the selective formation of CO_2 could result from the high oxidation activity of Au^0 on ceria particles, as observed on the reduced Au/CeO_2 catalyst, which would be high enough to fully oxidize the propene formed on the Au^0/Al_2O_3 active phase.

In the high temperature range, both the calcined and reduced $Au/CeO_2/Al_2O_3$ catalysts selectively form CO_2. This may suggest that, above 225 °C, the redox reaction on $Au^{\delta+}$ on ceria particles is able to gradually reduce $Au^{\delta+}$ to Au^0 and then to suppress the difference between the reduced and calcined catalyst, as attested by the drop in selectivity into propene at the benefit of CO_2 observed above 225 °C. Such gold reduction has been already observed during propene oxidation[6] with reduction starting around 100 °C and completed around 200 °C. We can then assume that the same behavior occurs with 2-propanol since we reasonably expect that the reducing power of 2-propanol is close to that of propene.

The stability of the catalysts towards 2-propanol conversion under air was examined at 50% conversion of 2-propanol for Au/CeO_2 and $Au/10CeO_2/Al_2O_3$ at 138 and 145 °C, respectively. Both catalysts exhibit a stable activity up to 24 hours of continuous run (Table 2).

Table 2 Catalytic results

	Activity[a] ($\times 10^4$ mol s^{-1} g_{Au}^{-1})	
Catalyst	Calcination	Reduction
Au/CeO_2	10.14[b]	11.22[b]
$Au/1.5CeO_2/Al_2O_3$	9.85	10.22
$Au/3CeO_2/Al_2O_3$	9.78	10.54
$Au/5CeO_2/Al_2O_3$	9.44	11.07
$Au/10CeO_2/Al_2O_3$	9.13	12.04
Au/Al_2O_3	8.9[b]	9.1[b]

[a] Activity measured at 125 °C. [b] After subtracting the contribution of the pure support.

4. Conclusions

Oxidation of 2-propanol over 1%Au/CeO_2, 1%Au/Al_2O_3 and 1%$Au/xCeO_2/Al_2O_3$ catalysts has been investigated. The total oxidation into CO_2 pathway involved the formation of acetone and propene as intermediates. Except for Au/CeO_2, three different reaction temperature regions can be distinguished. The low temperature region (50–150 °C) showed the exclusive 2-propanol dehydrogenation into acetone. Above 175 °C, the propene formation appeared to be the main reaction product at 225 °C on Au/Al_2O_3 and on calcined $Au/CeO_2/Al_2O_3$ catalysts. For Au/Al_2O_3, the temperature range for dehydration expanded up to 400 °C, due to the low activity of gold on alumina towards total oxidation.

The effects of activation treatment, ceria loading and the presence/absence of O_2 were studied. Whatever the catalyst activation procedure (calcination or reduction) the catalytic activity followed the order: $Au/CeO_2 > Au/xCeO_2/Al_2O_3 > Au/Al_2O_3$. For the $Au/xCeO_2/Al_2O_3$ catalysts, with increasing ceria loading, the catalytic activity decreased for calcination pre-treatment and increased for reduction pre-treatment likely due to the low activity of oxidized gold on ceria particles. Another interesting result is that although the Au/Al_2O_3 and $Au/CeO_2/Al_2O_3$ catalysts are not very good for total oxidation reaction, they are efficient towards the low temperature selective oxidation, *i.e.*, dehydrogenation of 2-propanol into acetone. Au on both supported and unsupported ceria samples exhibited stable catalytic activity for more than 24 hours without any deactivation at 125 °C.

Acknowledgements

The authors acknowledge the ANR (Agence Nationale pour la Recherche), which sponsored this work (ANR-BLANC07-2 183612).

References

1 M. A. Centeno, M. Paulis, M. Montes and J. A. Odriozola, *Appl. Catal., A*, 2002, **234**, 65.
2 S. Sciré, S. Minico, C. Crisafulli, C. Satriano and A. Pistone, *Appl. Catal., B*, 2003, **40**, 43.
3 D. Andreeva, P. Petrova, J. W. Sobczak, L. Ilieva and M. Abrashev, *Appl. Catal., B*, 2006, **67**, 237.
4 M. L. Jia, H. F. B. Zhaorigetu, Y. N. Shen and Y. F. Li, *J. Rare Earths*, 2008, **26**, 528.

5 B. Solsona, T. Garcia, R. Murillo, A. M. Mastral, E. N. Ndifor, C. E. Hetrick, M. D. Amiridis and S. H. Taylor, *Top. Catal.*, 2009, **52**, 492.
6 L. Delannoy, K. Fajerwerg, P. Lakshmanan, C. Potvin, C. Méthivier and C. Louis, *Appl. Catal., B*, 2010, **94**, 117.
7 P. Lakshmanan, L. Delannoy, V. Richard, C. Méthivier, C. Potvin and C. Louis, *Appl. Catal., B*, 2010, **96**, 117.
8 Q. Fu, A. Weber and M. F. Stephanopoulos, *Catal. Lett.*, 2001, **77**, 87.
9 R. Leppelt, B. Schumacher, V. Plzak, M. Kinnea and R. J. Behm, *J. Catal.*, 2006, **244**, 137.
10 M. M. Schubert, V. Plzak, J. Garche and R. J. Behm, *Catal. Lett.*, 2001, **76**, 143.
11 A. Trovarelli, *Catalysis by Ceria and Related Materials; Catalytic Science Series*, World Scientific Publishing Company, UK, 2002, vol. 2.
12 W. Deng, A. I. Frenkel, R. Si and M. F. Stephanopoulos, *J. Phys. Chem. C*, 2008, **112**, 12834.
13 R. Si and M. F. Stephanopoulos, *Angew. Chem., Int. Ed.*, 2008, **47**, 2884.
14 D. Widmann, R. Leppelt and R. J. Behm, *J. Catal.*, 2007, **251**, 437.
15 A. C. Gluhoi, N. Bogdanchikova and B. E. Nieuwenhuys, *J. Catal.*, 2005, **229**, 154.
16 M. Baron, O. Bondarchuk, D. Stacchiola, S. Shaikhutdinov and H.-J. Freund, *J. Phys. Chem. C*, 2009, **113**, 6042.
17 R. D. Shannon, *Acta Crystallogr., Sect. A: Cryst. Phys., Diffr., Theor. Gen. Cryst.*, 1976, **32**, 751–767.
18 L. H. Ahrens, *Geochim. Cosmochim. Acta*, 1952, **2**, 155–169.
19 M. Sugiura, M. Ozawa, A. Suda, T. Suzuki and T. Kanazawa, *Bull. Chem. Soc. Jpn.*, 2005, **5**, 78.
20 A. M. Venezia, G. Pantaleo, A. Longo, G. D. Carlo, M. P. Casaletto, F. L. Liotta and G. Deganello, *J. Phys. Chem. B*, 2005, **109**, 2821–2827.
21 S.-Y. Lai, Y. Qiu and S. Wang, *J. Catal.*, 2006, **237**, 303–313.
22 F. Serre, G. Garin, G. Belot and J. Maire, *J. Catal.*, 1993, **141**, 1.
23 S. Minico, S. Sciré, C. Crisafulli, R. Maggiore and S. Galvagno, *Appl. Catal., B*, 2000, **28**, 245.
24 S. Sciré, S. Minico, C. Crisafulli and S. Galvagno, *Catal. Commun.*, 2001, **2**, 229.
25 A. Trovarelli, *Catal. Rev. Sci. Eng.*, 1996, **38**, 439.
26 A. Piras, A. Trovarelli and G. Dolcetti, *Appl. Catal., B*, 2000, **28**, L77.
27 A. M. Arias, M. F. Garcia, L. N. Salamanca, R. X. Valenzuela, J. C. Conesa and J. Soria, *J. Phys. Chem. B*, 2000, **104**, 4038.
28 A. Gervasini and A. Auroux, *J. Catal.*, 1991, **131**, 190.
29 A. Gervasini, J. Fenyvesi and A. Auroux, *Catal. Lett.*, 1997, **43**, 219.
30 D. Haffad, A. Chambellan and J. C. Lavalley, *J. Mol. Catal. A: Chem.*, 2001, **168**, 153.
31 D. Kulkarni and I. E. Wachs, *Appl. Catal., A*, 2002, **237**, 121.
32 X. Gu, H. Chen and J. Shen, *Chin. J. Catal.*, 2003, **24**, 885.

